
Molten salt synthesis of a nanolaminated Sc₂SnC MAX Phase

LI You-Bing^{1,2}, QIN Yan-Qing^{1,2}, CHEN Ke^{1,2}, CHEN Lu^{1,2}, ZHANG Xiao^{1,2}, DING Hao-Ming^{1,2}, LI Mian^{1,2}, ZHANG Yi-Ming^{1,2}, DU Shi-Yu^{1,2}, CHAI Zhi-Fang^{1,2}, HUANG Qing^{1,2}

(1. Engineering Laboratory of Advanced Energy Materials, Ningbo Institute of Materials Technology and Engineering, Chinese Academy of Sciences, 315201, Ningbo, China; 2. Qianwan Institute of CNiTECH, Zhongchuangyi Road, Hangzhou bay District, Ningbo, Zhejiang, 315336)

Abstract: The MAX phases are a family of ternary layered material with both metal and ceramic properties, and it is also precursor materials for synthesis of two-dimensional MXenes. The theory predicted that there are more than 600 stable ternary layered MAX phases. At present, there are more than 80 kinds of ternary MAX phases synthesized through experiments, and few reports on MAX phases where M is a rare earth element. In this study, a new MAX phase Sc₂SnC with rare earth element Sc at the M sites was synthesized through the reaction sintering of Sc, Sn, and C mixtures. Phase composition and microstructure of Sc₂SnC were confirmed by X-ray diffraction, scanning electron microscopy and X-ray energy spectrum analysis. And structural stability, mechanical and electronic properties of Sc₂SnC was investigated via density functional theory. This study open a door for explore more unknown ternary layered rare earth compounds Re_{n+1}SnC_n (Re=Sc, Y, La-Nd, n=1) and corresponding rare earth MXenes.

Key words: MAX phases; Nanolaminated; Scandium; Density-functional theory calculation

The MAX phases are a family of nanolayered ternary carbides or nitrides with a hexagonal lattice structure (*P6₃/mmc*), the chemical formula is M_{n+1}AX_n (where M is an early transition metal; A belongs to group of 13-16; and X is carbon or/and nitrogen, n=1-3)^[1-3]. Generally, the heterodesmic feature of MAX phases contributes to a unique combination of both metallic and ceramic properties, and have been investigated as promising candidates for structural applications in many fields^[4-7]. Moreover, MAX phases are used as a precursor to synthesize two-dimensional (2D) MXene with many attractive physical and chemical properties, and show promise in a broad range of applications, notably electrochemical energy storage^[8-11]. Due to the continuing efforts from the scientific community, about 155 MAX phases have been reported so far; including some novel MAX phases that A-site elements are late transition metals^[12-16]. The theoretical studies have predicted around 665 ternary MAX phases that could be experimentally synthesized^[17], for example, the ones whose M site element is rare earth Sc.

As previous reported, Sc₂InC was listed as one of possible stable MAX phases^[1,3], where the structure, properties and potential applications are investigated via theoretical predictions^[18-20]; but not been experimentally identified yet. The Sc₂InC is expected to be a promising candidate for optoelectronic devices for the visible light and ultraviolet regions, as well as coating materials to avoid solar heating^[20]. In addition, theoretical calculations indicate that the Sc₂CT₂ (T= F, OH)

MXenes can be promising candidate materials for the next generation electronic devices^[21]. S. Kuchida et al^[22] focused on non-transition metal M₂AX compounds which embody Sc, Y, and Lu atoms in M site; however, only polycrystalline sample of Lu₂SnC was reported. As a result, the study of new MAX phases taking Sc as M site element is an intriguing and challenging work.

Now, the common synthesized of MAX phases methods are hot pressing (HP) and spark plasma sintering (SPS). Compared to HP and SPS, the molten salt method is a simple and cost-effective route for preparing MAX phase powders. As a high-temperature ionic solvent, the molten salt bath offers high solvation power and liquid environment for reactants that will greatly facilitate the mass transport and nucleation processes, thus need lower synthesis temperature and bold time^[23]. Some MAX phases (e.g. Ti₃SiC₂, Ti₃AlC₂, V₂AlC, Cr₂AlC) have been synthesized by molten salt method^[24-28]. In the present work, we synthesized a MAX phase of Sc₂SnC in molten salts environment where the Sc element belongs to rare earth. The crystal structure and chemical composition were confirmed by XRD and SEM-EDS, respectively. Furthermore, the structure stability, electronic structure and mechanical properties of Sc₂SnC are also be investigated via density functional theory (DFT).

1 Experimental

The raw materials used to prepare the MAX phase are scandium (Hunan Rare Earth Metal Materials Research Institute, Hunan, China; ~300 mesh, 99.5 wt.% purity), tin (Target Research Center of General Research Institute for Nonferrous Metals, Beijing, China, ~300 mesh, 99.5 wt.% purity), graphite (Qingdao Tianshengda Graphite Co. Ltd, Shandong, China; ~300 mesh, 99 wt.% purity), sodium chloride (Aladdin Industrial Co. Ltd, Shanghai, China; NaCl, 99.5 wt.% purity), potassium chloride (Aladdin Industrial Co. Ltd, Shanghai, China; KCl, 99.5 wt.% purity).

The powders were mixed in a stoichiometric ratio of Sc: Sn: C = 2: 1.1: 1 (Due to the melting point of Sn is relatively low, we increased the content ratio of tin for compensating the weight loss of tin at a high temperature, as in the preparation of $V_2(\text{Sn},\text{A})\text{C}$ MAX phases)^[16]. The starting powders of Sc, Sn and graphite are mixed with inorganic salt (NaCl + KCl), and the mole ratio of (Sc+Sn+C):(NaCl+KCl) was 1:10. After ground for 10 min, the powder mixture was put into an aluminum oxide boat, and then move to a tube furnace and heated to 1000 °C during 3 h with heating rate of 5 °C/min under argon atmosphere, respectively. After the reaction was finished, the product is washed, filtered and dried at 40 °C in vacuum; and the excess Sn element is removed by ferric chloride (Aladdin Industrial Co. Ltd, Shanghai, China; FeCl_3 , 99.5 wt.% purity).

The phase composition of the samples was determined by X-ray diffraction (XRD, D8 Advance, Bruker AXS, Germany) with $\text{Cu K}\alpha$ radiation. X-ray diffraction patterns were collected at a step size of 0.02° 2θ with a collection time of 1 s per step. The microstructure and chemical composition were observed by scanning electron microscopy (SEM, QUANTA 250 FEG, FEI, USA) equipped with an energy-dispersive spectrometer (EDS), and the EDS values were fitted by XPP (extended Puchou/Pichoir).

Density functional theory (DFT) calculations were programmed in the CASTEP code^[29-30], using the generalized gradient approximation (GGA) as implemented in the Perdew-Breke-Ernzerhof (PBE) functional^[31-32]. Phonon calculations were carried out to evaluate the dynamical stability using the finite displacement approach, as implemented in CASTEP^[33-34]. The equation $E=(E_{\text{broken}}-E_{\text{bulk}})/S$ ^[13] was adopted to calculate the cleavage energy E , where E_{bulk} and E_{broken} represent the total energies of bulk MAX and the cleav-

ing structures respectively with a 10 Å vacuum separation in the corresponding M and A atomic layers, and S is the cross-sectional surface area of the MAX phase materials. The Rietveld refinement of powder XRD pattern of Sc_2SnC was by Total Pattern Solution (TOPAS-Academic V6) software.

2 Results and discussion

2.1 Phase analysis of the Sc_2SnC

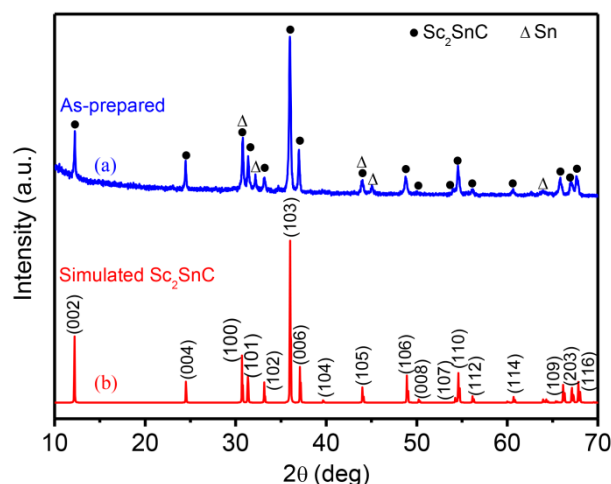


Fig. 1. Comparison of XRD patterns between (a) powders synthesized through the reaction between Sc, Sn, and C mixtures and (b) the simulated one of Sc_2SnC

Fig. 1a shows the XRD pattern of as-prepared powders synthesized at 1000 °C for 3 h, with characteristic peaks at $2\theta \sim 12^\circ$, $2\theta \sim 24^\circ$, and $2\theta \sim 36^\circ$, which neither belong to Sn nor other compounds, indicating a new MAX phase of Sc_2SnC was synthesized (also with minor amount of Sn metal as by-product). In comparison with experimental result, the simulated XRD pattern of Sc_2SnC in Fig. 1b, the peaks positioned at 12.174° , 24.517° , 36.277° , etc., consisting with the experimental peak positions in Fig. 1a, which further validates the formation of the new MAX phase Sc_2SnC .

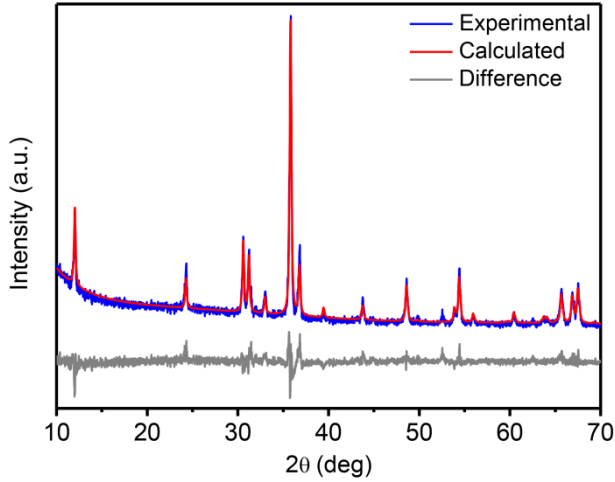


Fig. 2. Comparison between experimental (blue crosses) and calculated XRD (red line) pattern of Sc_2SnC .

Table 1. Atomic positions in Sc_2SnC determined from the Rietveld refinement

Site	Element	x	y	z	Symmetry	Wyckoff symbol
M	Sc	1/3	2/3	0.5786	3m	4f
A	Sn	1/3	2/3	0.25	$\bar{6}m2$	2d
X	C	0	0	0	$\bar{3}m$	2a

XRD pattern is important for phase identification and structure analysis. Due to no XRD pattern of Sc_2SnC is available from literature, the Rietveld refinement of powder XRD pattern of Sc_2SnC was conducted. As shown in Fig. 2, the blue crosses represent the experimental diffraction profile (the Sn metal was removed by FeCl_3 solution), while the red solid line denotes the theoretical pattern. The theoretical Bragg diffraction positions of Sc_2SnC are marked as green lines. The gray curve is the deviation between calculated and experimental XRD patterns. The obtained reliability factors are $R_p = 8.56\%$ and $R_{wp} = 11.19\%$, respectively; indicating good agreement between model and measured data. The space group of Sc_2SnC is $P6_3/mmc$ (No. 194), and the lattice constants measured from XRD pattern are $a = 3.3692 \text{ \AA}$ and $c = 14.6374 \text{ \AA}$, respectively. The difference between theoretical calculation and the Rietveld refinement is probably ascribed to the existence of defects in the crystal structure, as the case of V_2SnC in previous report^[35]. The atomic positions of Sc_2SnC determined from the Rietveld refinement are listed in Table 1.

2.2 Microstructural of the Sc_2SnC

It is well known that MAX phases crystallize in

hexagonal structures and their grains are generally layered hexagonal morphology^[1]. To confirm that Sc_2SnC has a similar microstructure, the microstructure of as-prepared powder was observed by SEM. It can be seen from Fig. 3a that Sc_2SnC exhibits the microstructure of typical thin hexagons. EDS equipped in SEM detected all constitutive elements (Sc, Sn and C) within these particles (shown in Fig. 3b). Although the EDS analysis is semi-quantitative and the accurate determination of light elements like C is difficult, the relative atomic ratio of (Sc:Sn:C) could be revealed by EDS as about (2:1:1), consistent with the stoichiometry of 211 MAX phases. The Elemental mapping of Sc, Sn and C corroborated that all of these three elements have the same distribution. The above results further confirmed that the new MAX phase compound Sc_2SnC is experimentally synthesized.

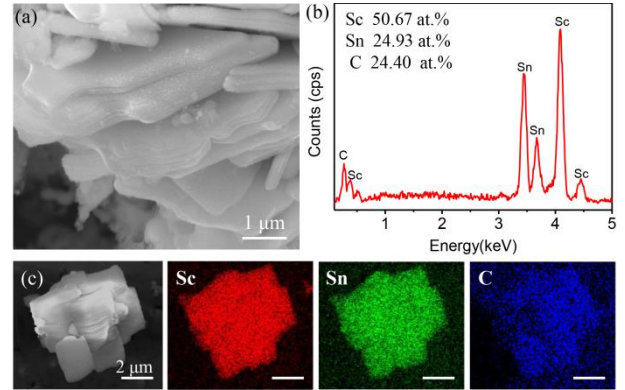


Fig. 3. (a) SEM image of Sc_2SnC . (b) The corresponding EDS spectrum indicated that particles contain Sc, Sn and C elements. (c) Elemental mapping clearing proving the uniform distribution

2.3 DFT results

The structural analysis of Sc_2SnC phase was carried out via DFT calculations. Fig. 4a shows the ternary-layered carbide crystal structure of Sc_2SnC ; and the calculated ΔH_{form} (Sc_2SnC) is -0.7167 eV , indicating stability of the Sc_2SnC phase. The lattice parameters, elastic constants and polycrystalline elastic modulus of Sc_2SnC , as well as for other Sn-containing MAX phases are listed in Table 2. From the DFT calculation result, the $a = 3.3686$, $c = 14.6532 \text{ \AA}$, which was very close to experimental results. The mechanical stability of Sc_2SnC was justified from the Born stability criteria^[36]: $C_{11} > 0$, $C_{11} - C_{12} > 0$, $C_{44} > 0$, $(C_{11} - C_{12})C_{33} - 2C_{13} > 0$. Besides, the dynamical stability of Sc_2SnC can also be identified from the phonon dispersion curves in Fig. 4b. The results performed by theoretical calculations are consistent with experiments. However, compared with other MAX phases (listed in Table 2), it is found

that they have lower values of elastic constants (i.e. C_{11} , C_{33} , C_{44} , and C_{66}).

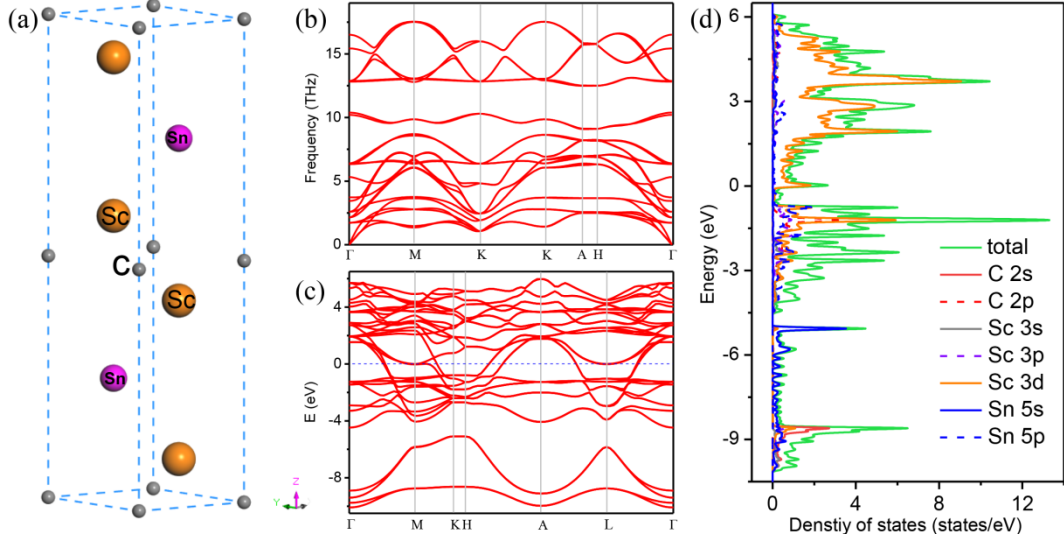


Fig. 4. (a) Crystal structure of Sc_2SnC ; (b) Calculated phonon dispersion of Sc_2SnC ; (c) Band structure of Sc_2SnC ; (d) Projected density of Sc, Sn, and C atom states.

Table 2. Theoretically predicted Lattice parameters (\AA), calculated elastic constants, C_{ij} (GPa), bulk modulus, B (GPa), shear modulus, G (GPa), and Young's modulus, E (GPa), Pugh ratio, G/B, and Poisson ratio, ν , of Sc_2SnC , V_2SnC , Ti_2SnC , Zr_2SnC , Hf_2SnC , and Nb_2SnC .

Compound	a (\AA)	c (\AA)	C_{11}	C_{12}	C_{13}	C_{33}	C_{44}	C_{66}	B	G	E	G/B	ν	Ref.
Sc_2SnC	3.368	14.653	197	63	47	182	67	53	100	63	157	0.630	0.238	This work
V_2SnC	3.134	12.943	336	126	122	304	85	105	190	95	244	0.500	0.286	35
Ti_2SnC	3.136	13.641	337	86	102	329	169	126	176	138	328	0.784	0.188	39
Zr_2SnC	3.352	14.681	269	80	107	290	148	94	157	110	368	0.700	0.215	39
Hf_2SnC	3.308	14.450	330	54	126	292	167	138	173	132	316	0.763	0.195	39
Nb_2SnC	3.244	13.754	341	106	169	321	183	118	209	126	314	0.603	0.250	39

The relative small value of C_{33} indicates the compound is more compressible along the c-axis compared to other compounds studied; while low C_{44} indicates being subject to shear deformation along $[11\bar{2}0]$ (0001); and small C_{66} probably means lower resistance to shear in the $\langle 110 \rangle$ direction^[20,35,37]. The low shear deformation of Sc_2SnC is also reflected from shear modulus G, which represents the resistance to shape change of the polycrystalline material^[38]. The calculated value of $G/B > 0.5$ indicates that the phase is brittle in nature following Pugh's criterion. Furthermore, the obtained value of ν (0.238) for Sc_2SnC shows that it is located at the boundary between covalent and ionic materials. The calculated band structure of Sc_2SnC and the projected

density of states (DOS) of Sc, Sn, and C atoms with k-points are shown in Fig. 4c and Fig. 4d, respectively. Similar to other MAX phases and MAX phase-like compounds, Sc_2SnC exhibits metallic nature; and the overlapping between valence and conduction bands across the Fermi level also reveals the presence of metallic bonding, which can be treated as the origin of the quasi-ductility of Sc_2SnC (Fig. 4c). As can be seen from Fig. 4d, it can be observed that the Sc-3d electrons are mainly contributing to the DOS at the Fermi level, and should be involved in the conduction properties; while the contributions from.

3 Conclusions

In conclusion, a new MAX phase was successfully synthesized for the first time by heating the Sc, Sn, and C raw powder mixtures. The XRD data of Sc₂SnC is useful for further phase identification and structure analysis; and Sc₂SnC exhibits a typical laminar microstructure similar to other MAX phases. The first-principle calculations were employed to further study structure stability of Sc₂SnC MAX phase, and the results showed that Sc₂SnC is metallic in nature where the contribution from Sc-3d states dominates the electronic conductivity at the Fermi level. This work implies the great potential of the ternary rare-earth metal carbide Re_{n+1}SnC_n (Re=Sc, Y, La-Nd, n = 1) family waiting for further explore. More importantly, the introduction of rare earth elements can give the special properties of MAX phases, and can be used as a precursor material for preparing rare-earth MXenes.

References

- [1] BARSOUM M W. The M_{N+1}AX_N phases: a new class of solids; thermodynamically stable nanolaminates. *Progress in Solid State Chemistry*, 2000, **28**(1): 201-281.
- [2] SOKOL M, NATU V, KOTA S, *et al.* On the chemical diversity of the MAX phases. *Trends in Chemistry*, 2009, **1**(2): 210-223.
- [3] EKLUND P, BECKERS M, JANSSON U, *et al.* The M_{n+1}AX_n phases: materials science and thin-film processing. *Thin Solid Films*, 2010, **518**(8): 1851-18782.
- [4] WHITTLE K R, BLACKFORD M, AUGHTERSON M R, *et al.* Radiation tolerance of M_{n+1}AX_n phases, Ti₃AlC₂ and Ti₃SiC₂. *Acta Materialia*, 2010, **58**(13): 4362-4368.
- [5] FASHANDI H, DAHLQVIST M, LU J, *et al.* Synthesis of Ti₃AuC₂, Ti₃Au₂C₂ and Ti₃IrC₂ by noble metal substitution reaction in Ti₃SiC₂ for high-temperature-stable Ohmic contacts to SiC. *Nature Materials*, 2017, **16**(8): 814-818.
- [6] WARD J, BOWDEN D, PRESTAT E, *et al.* Corrosion performance of Ti₃SiC₂, Ti₃AlC₂, Ti₂AlC and Cr₂AlC MAX phases in simulated primary water conditions. *Corrosion Science*, 2018, **39**: 444-453.
- [7] ZHU Y, ZHOU A, JI Y, *et al.* Tribological properties of Ti₃SiC₂ coupled with different counterfaces. *Ceramics International*, 2012, **41**(5): 6950-6955.
- [8] NAGUIB M, KURTOGLU M, PRESSER V, *et al.* Two-dimensional nanocrystals produced by exfoliation of Ti₃AlC₂. *Advanced Materials*, 2011, **23**(37): 4248-4253.
- [9] LUKATSKAYA M R, MASHTALIR O, REN C E, *et al.* Cation intercalation and high volumetric capacitance of two-dimensional titanium carbide. *Science*, 2013, **341**(6153): 1502-1505
- [10] ANASORI B, LUKATSKAYA M R, GOGOTSI Y. 2D metal carbides and nitrides (MXenes) for energy storage. *Nature Reviews Materials*, 2017, **2**(2): 16098.
- [11] LI Y B, SHAO H, LIN Z F, *et al.* A general lewis acidic etching route for preparing MXenes with enhanced electrochemical performance in non-aqueous electrolyte. *Nature Materials*, 2020, **19**(8): 894-899.
- [12] NECHICHE M, GAUTHIER-BRUNET V, MAUCHAMP V, *et al.* Synthesis and characterization of a new (Ti_{1-x}Cu_x)₃(Al,Cu)₂ MAX phase solid solution. *Journal of the European Ceramic Society*, 2019, **37**(2): 459-466.
- [13] LI M, LU J, LUO K, *et al.* Element replacement approach by reaction with lewis acidic molten salts to synthesize nanolaminated MAX phases and MXenes. *Journal of the American Chemical Society*, 2019, **141**(11): 4730-4737.
- [14] LI Y, LI M, LU J, *et al.* Single-atom-thick active layers realized in nanolaminated Ti₃(Al_xCu_{1-x})C₂ and its artificial enzyme behavior. *ACS Nano*, 2019, **13**(8): 9198-9205.
- [15] DING H, LI Y B, LU J, *et al.* Synthesis of MAX phases Nb₂CuC and Ti₂(Al_{0.1}Cu_{0.9})N by A-site replacement reaction in molten salts. *Materials Research Letters*, 2019, **7**(12): 510-516.
- [16] LI Y B, LU J, LI M, *et al.* Multielemental single-atom-thick A layers in nanolaminated V₂(Sn,A)C (A = Fe, Co, Ni, Mn) for tailoring magnetic properties. *Proceedings of the National Academy of Sciences of the United States of America*, 2020, **117**(2): 820-825.
- [17] ARYAL S, SAKIDJA R, BARSOUM M W, *et al.* A genomic approach to the stability, elastic, and electronic properties of the MAX phases. *Physical Status Solidi*, 2014, **251**(8): 1480-1497.
- [18] BOUHEMADOU A, KHENATA R, KHAROUBI M, *et al.* First-principles study of structural and elastic properties of Sc₂AC (A=Al, Ga, In, Tl). *Solid State Communications*. 2008, **146**(3-4): 175-180.
- [19] COVER M F, WARSCHKOW O, BILEK M M, *et al.* A comprehensive survey of MAX phase elastic properties. *Journal of Physics: Condensed Matter*, 2009, **21**(30): 305403.
- [20] CHOWDHURY A, ALI M A, HOSSAIN M. M, *et al.* Predicted MAX phase Sc₂InC: dynamical stability, vibrational and optical properties, *Physical Status Solidi*, 2018, **255**(3): 1700235
- [21] ZHA X H, REN J C, FENG L, *et al.* Bipolar magnetic semiconductors among intermediate states during the conversion from Sc₂C(OH)₂ to Sc₂CO₂ MXene. *Nanoscale*, 2018, 10(18): 8763-8771.
- [22] KUCHIDA S, MURANAKA T, KAWASHIMA K, *et al.* Superconductivity in Lu₂SnC. *Physica C: Superconductivity*, 2013, **494**: 77-79.
- [23] LIU X, FECHLER N, ANTONIETTI M. Salt melt synthesis of ceramics, semiconductors and carbon nanostructures. *Chemical Society Reviews*, 2013, **42**(21): 8237-8265.
- [24] WANG B, ZHOU A, HU Q, *et al.* Synthesis and oxidation resistance

-
- of V_2AlC powders by molten salt method. *International Journal of Applied Ceramic Technology*, 2017, **14(5)**: 873-879.
- [25] TIAN W-B, WANG P-L, KAN Y-M, *et al.* Cr_2AlC powders prepared by molten salt method. *Journal of Alloys and Compounds*, 2008, **461(1-2)**: L5-L10.
- [26] GALVIN T, HYATT N C, RAINFORTH W M, *et al.* Molten salt synthesis of MAX phases in the Ti-Al-C system. *Journal of the European Ceramic Society*, 2018, **38(14)**: 4585-4589.
- [27] GUO X, WANG J, YANG S, *et al.* Preparation of Ti_3SiC_2 powders by the molten salt method. *Materials Letters*, 2013, **111**: 211-213.
- [28] ROY C, BANERJEE P, BHATTACHARYA S. Molten salt shielded synthesis (MS3) of Ti_2AlN and V_2AlC MAX phase powders in open air. *Journal of the European Ceramic Society*, 2020, **40(3)**: 923-929.
- [29] CLARK S J, SEGALL M D, PICKARD C J, *et al.* First principles methods using CASTEP. *Zeitschrift fur Kristallographie-Crystal-line Materials*, 2005, **220**: 567-570.
- [30] SEGALL M, LINDAN P J, PROBERT M J, *et al.* First-principles simulation: ideas, illustrations and the CASTEP code. *Journal of Physics: Condensed Matter*, 2002, **14**: 2717-2744.
- [31] PERDEW J P, BURKE K, ERMZERHOF M. Generalized gradient approximation made simple. *Physical Review Letters*, 1996, **77(18)**: 3865-3868.
- [32] VANDERBILT D. Soft self-consistent pseudopotentials in a generalized eigenvalue formalism. *Physical Review B*, 1990, **41(11)**: 7892-789.
- [33] FRANK W, ELSASSER C, FAHNLE M. Ab initio force-constant method for phonon dispersions in alkali metals. *Physical Review Letters*, 1995, 74(10): 1791-1794.
- [34] PARLINSKI K, LI Z Q, KAWAZOE Y. First-principles determination of the soft mode in cubic ZrO_2 . *Physical Review Letters*, 1997, **78(21)**: 4063-4066.
- [35] XU Q, ZHOU Y, ZHANG H, *et al.* Theoretical prediction, synthesis, and crystal structure determination of new MAX phase compound V_2SnC . *Journal of Advanced Ceramics*, 2020, **29(4)**: 481-492.
- [36] BORN M, MISRA R D. On the stability of crystal lattices. *Mathematical Proceedings of the Cambridge Philosophical Society*, 1940, **36(4)**: 466-478.
- [37] KOC H, OZISIK H, DELIGOZ E, *et al.* Mechanical, electronic, and optical properties of Bi_2S_3 and Bi_2Se_3 compounds: first principle investigations. *Journal of Molecular Modeling*, 2014, **20(4)**: 2180.
- [38] PUGH S F. Relations between the elastic moduli and the plastic properties of polycrystalline pure metals. *The London, Edinburgh, and Dublin Philosophical Magazine and Journal of Science*. 1954, **45(367)**: 823-843
- [39] KANOUN M B, GOUNRI-SAID S, RESHAK A H. Theoretical study of mechanical, electronic, chemical bonding and optical properties of Ti_2SnC , Zr_2SnC , Hf_2SnC and Nb_2SnC . *Computational Materials Science*, 2009, **47(2)**: 491-500.